Seismic performance of slopes in northern Canada

Behrang Dadfar & M. Hesham El Naggar
Department of Civil and Environmental Engineering, Western University, London, Ontario, Canada
Miroslav Nastev
Geological Survey of Canada, Natural Resources Canada, Quebec City, Quebec, Canada

ABSTRACT
Infrastructures in northern Canada are potentially exposed to earthquake-induced slope instabilities requiring assessment of the seismic performance of natural slopes. Active layer detachments are the most common types of identified landslides, where terrain instability and downward movement of the active permafrost layer can be triggered by seismic excitation. This research aims at developing a framework for probabilistic slope stability analysis that accounts for the specific geological settings in the permafrost regions. Slope geometry, soil properties and ground motion uncertainties are incorporated in the model and the probabilities of weakening and inertial instabilities are investigated.

1 INTRODUCTION

In permafrost regions, an active layer represents the surficial layer of soils located on the permafrost table that is subject to annual freeze-thaw cycles. Its thickness varies between a few centimeters to few meters (Johnston 1981). In northern Canada, the active layer is comprised mainly of unconsolidated fine-grained sediments (Aylsworth et al. 2000), which together with rock outcrops cover extensive areas of the permafrost regions. Active layer detachment (ALD) is the most common type of landslides that has been identified in these areas (Dyke 2004, Lipovsky and Huscroft 2006). An ALD represents the downslope motion of the thawed surficial layer sliding over the permafrost table. ALD occurs when the thickness of the active layer increases and/or the pore-water pressure attains critical values. These conditions may develop as a consequence of different factors, such as climate warming, loss of vegetation cover, fire, and intensive rainfalls (Dyke 2000). In addition, earthquakes can also cause slope instabilities. Considerable parts of the permafrost regions in Canada, such as Southwestern Yukon, the Mackenzie and Richardson Mountains, and beneath the Beaufort Sea are prone to earthquakes (Hyndman et al. 2005, Adams et al. 2015). Seismic waves can trigger two types of instabilities, i.e., inertial instabilities (induced inertial forces) and weakening instabilities (excess pore-water pressure build-up that weakens soil shear strength).

In this study, the probability of occurrence of earthquake-induced ALDs is determined by Monte Carlo technique. The peak ground acceleration (PGA) of the scenario earthquake is characterized by the source-to-site distance (R) and moment magnitude (M_w). The geological settings of the Mackenzie Valley as an important corridor for the construction of the energy-related infrastructures are considered. Figure 1 schematically illustrates the problem together with a few significant parameters.

2 WEAKENING INSTABILITIES

Based on the classifications of Youd and Perkins (1978), the unconsolidated surficial soils of the Mackenzie Valley (including till, lacustrine, glaciofluvial, colluvial, and alluvial fine-grained sediments), under saturated conditions are considered to have low to moderate susceptibility to liquefaction.

According to Boulanger and Idriss (2006), fine-grained soils with plasticity index (PI) smaller than 7 show sand-like behaviour and can be liquefied. Extensive liquefaction was observed in fine-grained soils of the Mabel Creek area (Alaska, USA) after the 2002 M_w7.9 Denali earthquake (Zhang 2009). Lewkowicz and Harris (2005) reported a PI range of 2-30 for the samples collected from a number of locations in the Fosheim Peninsula and the Mackenzie Valley (Northwest Territories, Canada). As well, silty clay and clayey silt have been observed within a corridor east of the Mackenzie River (Wang et al. 2005). These are the rationales for studying the likelihood of weakening instabilities.

To evaluate the triggering condition for liquefaction, the factor of safety against liquefaction (FS_L) should be calculated. FS_L is given by:

$$FS_L = \frac{CRR}{CSR} \quad [1]$$

where, CRR and CSR are the cyclic resistance and the cyclic stress ratios, respectively. The former ratio indicates the soil resistance against liquefaction, whereas the latter represents the average shear stress induced by an earthquake.

The cyclic resistance ratio (CRR) can be evaluated using SPT values:

$$CRR = C_m . C_s . C_p . (CRR)_{M_w 7.5} \quad [2]$$

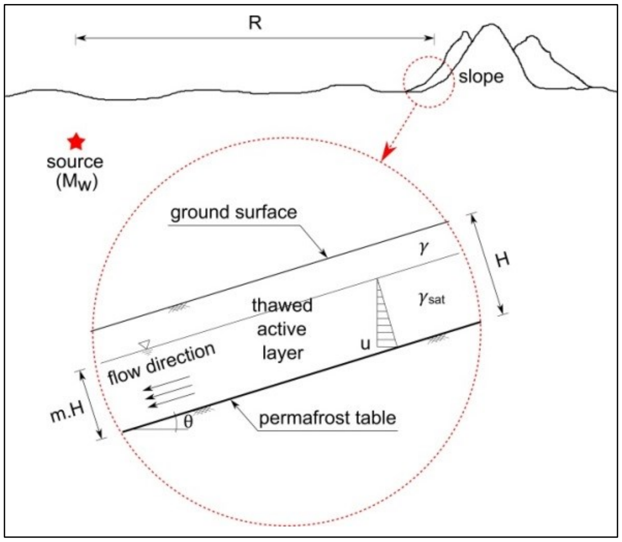

Figure 1. Schematic of the effect of a scenario earthquake on slopes in a permafrost region with infinite slope model parameters.

in which, $(CRR)_{Mw7.5}$ is a function of the normalized SPT blow counts of clean sand, $(N_1)_{60CS}$, for seismic event with M_w7.5 (Figure 2), and C_m, C_s, and C_p are the respective correction factors of earthquake magnitude, sloping ground, and soil plasticity. The first two parameters of Equation 2 are discussed in details by Youd et al. (2001) and the last one is introduced by Ishihara (1993). It should be noted that due to the large scatter in the experimental data, currently there is no consensus on the appropriate values of C_s. However, in the absence of precise methods this simple procedure is being used in engineering practice.

For the cyclic stress ratio (CSR), on the other hand, Seed and Idriss (1971) presented the following equation:

$$CSR = 0.65\left(\frac{\sigma_v}{\sigma_v'}\right).PGA.r_d \quad [3]$$

where, σ_v and σ'_v are the total and effective vertical stresses at the depth of interest, PGA is the peak ground acceleration given as a fraction of g, and r_d is the reduction factor of depth.

When FS_L<1, the slope may experience weakening instability provided that the factor of safety against weakening instability (FS_W) is smaller than 1:

$$FS_W = \frac{S_u}{H[(1-m)\gamma + m\gamma_{sat}]\sin\theta} \quad [4]$$

In this equation, H is the thickness of the active layer, m is the portion of the active layer's depth below the water table, and S_u is the undrained shear strength of the soil.

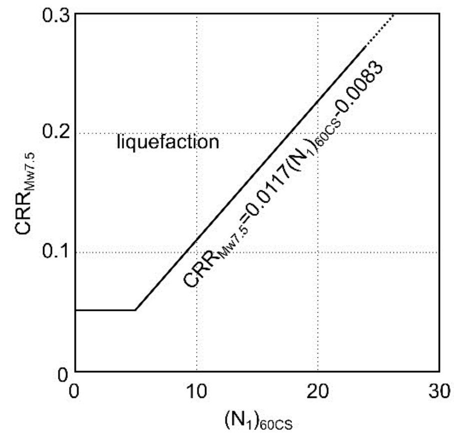

Figure 2. Simplified relationship between the cyclic resistance ratio (CRR) and the normalized SPT value of clean sand for an M_w7.5 earthquake, developed based on Youd et al. (2001).

S_u has been estimated by the equations proposed by Olson and Stark (2002) for the non-plastic silts (i.e., 0<PI<4 in this study) and Mesri (1975) for clays (i.e., 4<PI<7 that represents the transitional zone between sand-like and clay-like soil behaviours in this study):

$$S_u = \begin{cases} [0.03 + 0.0075(N_1)_{60}]\sigma_v' & 0 < PI < 4 \\ 0.22\sigma_v' & 4 \le PI < 7 \end{cases} \quad [5]$$

In these equations, σ'_v is the vertical effective stress at the studied depth.

3 INERTIAL INSTABILITIES

The parallel-to-slope component of the ground acceleration, a(t), may exceed the critical acceleration at the potential slip surface, a_c, several times during the ground shaking. The Newmark's sliding block approach is applied herein to estimate the co-seismic permanent slope deformations. It is based on a cumulative sum of the relative displacements of the soil block and the sliding surface over the times when the critical acceleration is exceeded. This procedure requires setting a value for a_c, and then computing the double integration of a(t) over the "exceedance" durations. If the resulted "Newmark displacement", D_N, exceeds a threshold displacement, D_{NT}, the slope can be considered as unstable.

Jibson et al. (2000) calibrated the Newmark's approach by comparing the field observations of the landslides triggered by the 1994 Northridge earthquake with the Newmark displacements computed for that event. They concluded that the probabilities of inertial instabilities equal to 83% and 96% correspond to the Newmark displacements smaller than 10 and 15 cm, respectively. So far, different values for D_{NT} ranging from 1 cm to 15 cm based on the likelihood of damage, depth, type and the location of landslide have been proposed by Wieczorek et al. (1985), Keefer and Wilson (1989), Blake et al. (2002), California Geological Survey (2008), and Jibson and Michael (2009). Jibson and Michael (2009) suggested the range of 5 to 15 cm for D_{NT} corresponding to the high likelihood of the occurrence of shallow landslides in Anchorage, Alaska. As well, Keefer and Wilson (1989) derived the threshold value of 10 cm for coherent landslides. Therefore, in the absence of detailed information regarding the local soil behaviour, D_{NT}=10 cm was considered which is also an average of those reported in the literature.

To overcome the difficulties of the implementation of double integration procedure for the computation of D_N, several regression models have been proposed (Sarma 1988, Ambraseys and Menu 1988, Jibson et al. 1998, and Jibson 2007). In this study, the expression developed by Jibson (2007) is employed:

$$\log D_N = 2.401 \log I_a - 3.481 \log a_c - 3.230 \pm \sigma \qquad [6]$$

where, D_N is given in terms of the Arias intensity, I_a in m/sec, and the critical acceleration a_c as a fraction of g. In Equation 6, σ=0.656 and represents the standard deviation of the regression model. To calculate D_N, I_a and a_c should be known. I_a can be obtained from the following Arias intensity attenuation relationship developed by Wilson and Keefer (1985):

$$\log I_a = M_w - 2 \log R - 4.1 \qquad [7]$$

The critical acceleration of an infinite slope with angle θ and a planar slip surface parallel to the ground surface, as depicted in Figure 1, can be written as:

$$a_c = \frac{\tan\theta}{1+\tan\theta\tan\phi'}(FS_I - 1)g \qquad [8]$$

where, Φ' is the effective soil friction angle, and FS_I is the static factor of safety. The parallel-to-slope and perpendicular-to-slope components of horizontal ground acceleration are accounted for in deriving Equation 8.

Using the slope parameters shown in Figure 1 and applying the limit equilibrium method, FS_I can be written as:

$$FS_I = \frac{c' + \{H[(1-m)\gamma + m\gamma_{sat}]\cos\theta - u\}\tan\phi'}{H[(1-m)\gamma + m\gamma_{sat}]\sin\theta} \qquad [9]$$

where, c' is the effective soil cohesion, and u is the pore-water pressure at the potential slip surface.

4 EARTHQUAKE PARAMETERS

To evaluate the PGA for a scenario earthquake of magnitude M_w at a site with distance R from the epicentre, a site-consistent ground motion prediction equation (GMPE) is required. In this study, the GMPE developed by Boore et al. (1997) for the Western North America is employed. The standard deviation of Ln(PGA) in this model is 0.468. The distance R in Boore et al. and the distance applied in Equation 7 have the same definition, i.e., the closest horizontal distance from the site to the vertical projection of the rupture plane (Joyner and Boore 1981).

The average shear wave velocity of the top 30 m at the site, V_{s30}, characterizes the local site conditions in the considered GMPE. In this study, due to the presence of permafrost (with the average shear-wave velocity of up to 1500 m/sec) beneath the site, V_{s30}=620 m/sec that represents Type C soil in the National Building Code of Canada (2010) is applied to the GMPE.

The projection of horizontal PGA along the slope aspect was calculated by:

$$PGA_{slope} = PGA_{GMPE}.\cos\alpha \qquad [10]$$

where, α is a random variable that indicates the angle between horizontal excitations and slope aspect (dip direction).

5 PORE-WATER PRESSURE

The effect of pore-water pressure, u, on the weakening and inertial instabilities is incorporated through Equations 3 and 9, respectively. Normally, in these equations u is the hydrostatic pore-water pressure and for the infinite slope and flow direction shown in Figure 1 it is equal to:

$$u = mH\gamma_w \cos\theta \qquad [11]$$

In an active layer with fine-grained soil, however, when the rate of thawing is higher than the rate of water drainage and consolidation, some excess pore-water pressure builds up. Morgenstern and Nixon (1971) explained this phenomenon referred to as "thaw-consolidation" with the following equation for the excess-pore water pressure, Δu:

$$\Delta u = \frac{mH(\gamma_{sat} - \gamma_w)\cos\theta}{1 + \frac{1}{2R_{tc}^2}} \qquad [12]$$

where, R_{tc} is the thaw-consolidation ratio and depends on a heat conductivity-related constant, α_h, and the coefficient of consolidation, c_v, of the thawing soil:

$$R_{tc} = \frac{\alpha_h}{2\sqrt{c_v}} \qquad [13]$$

The total pressure under thaw-consolidation phenomenon can be obtained by adding Δu to the hydrostatic pore-water pressure (Equation 11).

6 MONTE CARLO SIMULATIONS

The final step in the proposed framework for assessment of the probabilities of failure in the slopes underlain by permafrost consists of applying the Monte Carlo simulation technique. A procedure was developed to deal with the two potential modes of failure, i.e., weakening and inertial instabilities. A flowchart describing this procedure is shown in Figure 3. As can be seen, initially the likelihood of weakening instability is screened by verifying the soil PI. In cases where PI is smaller than 7 (sand-like behaviour), the factor of safety against liquefaction (FS_L) should be calculated first. If FS_L<1, the factor of safety against weakening instability (FS_W) smaller than 1 indicates the occurrence of weakening instability. Alternatively, for FS_W greater than 1 the slope can be considered as safe at least against the weakening instabilities. If the latter condition occurs, the likelihood of inertial instability will be checked by comparing the Newmark displacement with the threshold value which was considered 10 cm.

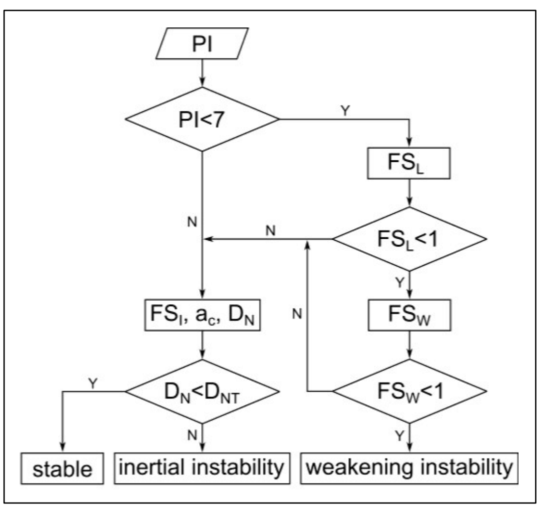

Figure 3. The procedure developed in this study to determine the slope stability condition.

The input variables of Monte Carlo simulations are given in Table 1. The mean values and coefficients of variation (COV) of the input parameters were assumed based on the values reported in the literature, e.g., by Lewkowicz (1990) and Lewkowicz and Harris (2005), and the guidelines of Phoon and Kulhawy (1999). All input variables except for c' and Φ' are independent. Uzielli et al. (2007) proposed a range of -0.75 to -0.25 for the coefficient of correlation between c' and Φ'. In this study, the coefficient of correlation was considered -0.5, the average of the proposed range.

In each simulation 100,000 random realizations were generated. However, only those with the static factor of safeties (FS_I) larger than 1 where involved in the slope stability computations, because they were in static equilibrium before earthquake. Effects of θ, M_w, R and R_{tc} as the most significant parameters were studied.

6.1 Effect of Slope Inclination Angle

Figure 4 shows the variation of the probability of slope failure with the change of slope angle. The probability of failure is defined as the sum of the probabilities of weakening and inertial instabilities. In this study, an M_w6.5 earthquake with a source-to-site distance of 40 km was assumed. Also, thawing condition was considered normal, i.e., R_{tc}=0.

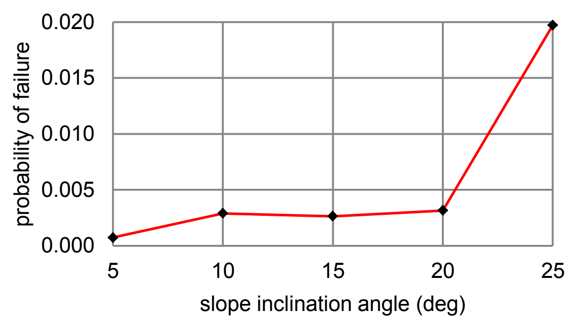

Figure 4. Variation of the probability of failure with the change of slope angle.

Up to θ=15°, the probability of inertial instability is zero and from this point onward, it starts increasing. The corresponding probabilities of weakening and inertial instabilities are presented in Table 2. In this table, P(WI) is the probability of weakening instability, P(II) is the probability of inertial instability, P(F) is the probability of failure, and β is the reliability index, defined as:

$$\beta = -\Phi^{-1}[P(F)] \qquad [14]$$

where, Φ^{-1}[.] is the inverse standard normal cumulative function.

From the reliability indices given in Table 2, the performance of the slopes with the respective inclination angles of 5 to 25 degrees is predicted to be "above average" to "poor" according to the US Army Corps of Engineers (1997).

Table 1. Input variables of Monte Carlo simulations.

Variable		Probabilistic			Deterministic	Remarks
		Mean	COV[1] (%)	Distribution		
slope:	θ (deg)	-	-	-	5, 15, 25	-
	H (m)	1.0	30	lognormal	-	-
	m	0.75	5	beta	-	0.5≤m≤1.0
soil:	γ_d (kN/m^3)	16	9	lognormal	-	-
	c' (kPa)	2.5	20	lognormal	-	cross-correlated to ϕ'
	ϕ' (deg)	26	10	lognormal	-	cross-correlated to c'
	$(N_1)_{60}$	5	45	lognormal	-	-
	FC[2] (%)	-	-	-	70	-
	PI (%)	16	40	beta	-	2≤PI≤30
	D_r (%)	-	-	-	40	-
	R_{tc}	-	-	-	0.0, 1.5, 3.0	-
	D_{NT} (cm)	-	-	-	10	-
ground motion:	M_w	-	-	-	5.5, 6.5, 7.5	-
	R (km)	-	-	-	10, 40, 80	-
	α[3] (deg)	45	-	uniform	-	0≤α≤90

[1]coefficient of variation
[2]fines content
[3]the angle between horizontal excitations and slope aspect (dip direction)

Table 2. The slope instability probabilities and the reliability index in terms of θ.

θ (deg)	P(WI)	P(II)	P(F)	β
5	0.00072	0.00000	0.00072	3.19
10	0.00289	0.00000	0.00289	2.76
15	0.00263	0.00000	0.00263	2.79
20	0.00201	0.00114	0.00315	2.73
25	0.00147	0.01825	0.01972	2.06

6.2 Effect of Earthquake Parameters

The GMPE equation used in this study (Boore et al., 1997) is valid for the moment magnitudes between 5.5 and 7.5. Therefore, the effect of three values of M_w on slope instability was studied. Results of this study are plotted in Figure 5.

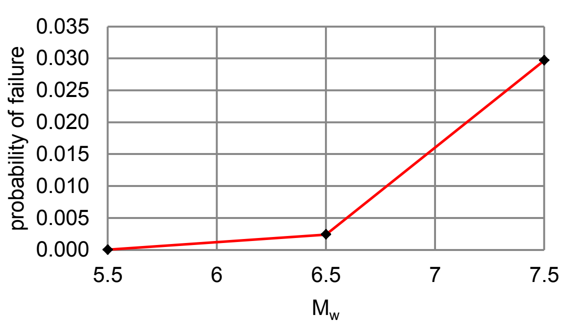

Figure 5. Variation of the probability of failure with the change of earthquake moment magnitude.

In this study, the slope angle was 15°, the source-to-site distance was 40 km, and the thaw-consolidation ratio was zero.

In all three scenarios, Monte Carlo realizations did not predict any inertial instabilities. However, this may not be the case for a different combination of input parameters.

The effect of source-to-site distance, R, on the probability of failure is shown in Figure 6. As it was expected, damage level decreases with the increase of distance to the seismic source. Again, only weakening instabilities were observed in the simulations. Here, the slope angle, moment magnitude and thaw-consolidation ratio were 15°, 6.5 and 0, respectively.

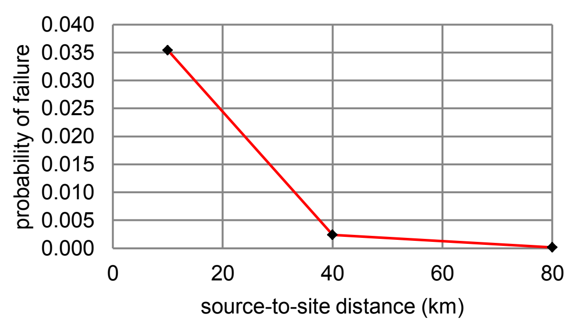

Figure 6. Variation of the probability of failure with the source-to-site distance.

6.3 Effect of Thaw-Consolidation Phenomenon

The condition when the thaw-consolidation ratio is determined as larger than 1 is equivalent to the existence of some excess pore-water pressure in the thawed active layer before the start of the ground shaking. Theoretically, this should increase the likelihood of slope instability. To study the effect of this phenomenon on the seismic behavior of the northern slopes, three values for R_{tc} were considered, 0, 1.5 and 3.

Similar to the previous parametric studies, the remaining important parameters were kept constant, i.e., the effect of an M_w6.5 event occurring at a distance equal 40 km from a slope with θ=15° was simulated. The results are shown in Figure 7.

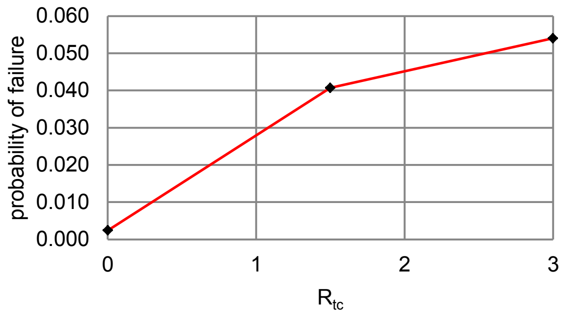

Figure 7. Variation of the probability of failure with the thaw-consolidation ratio.

The respective probabilities are given in Table 3 to assess the contribution of the two modes of instability. As can be seen, both failure modes have almost equal contributions in the considered cases when R_{tc} is greater than 0. The contribution of weakening and inertial instabilities will change with the change of other parameters. The increase of R_{tc}, however will lead to the increase of the probability of failure.

Table 3. The slope instability probabilities and the reliability index in terms of R_{tc}.

R_{tc}	P(WI)	P(II)	P(F)	β
0.0	0.00263	0.00000	0.00263	2.79
1.5	0.01859	0.01068	0.02927	1.89
3.0	0.02513	0.01721	0.04234	1.72

6.4 The Worst-Case Scenario

According to the results of previous sections, the worst-case scenario was simulated for the slopes with inclination angles between 5 to 25 degrees, located at a distance of 10 km from the epicenter of an M_w7.5 earthquake, while the active layers have thaw-consolidation ratios of 3. The results are shown in Figure 8. As can be seen, the probabilities of failure, compared to those shown in Figure 4, have considerably increased.

The reliability indices corresponding to the probabilities of failure are given in Table 4. The performance of slopes under this scenario according to the classifications of the US Army Corps of Engineers is considered “unsatisfactory” and “hazardous”.

Accounting for the simultaneous occurrence of an earthquake and the thaw-consolidation phenomenon may currently seem far-fetched; however, with the increasing trend of global warming over the time, this may not be regarded as an impossible scenario in future.

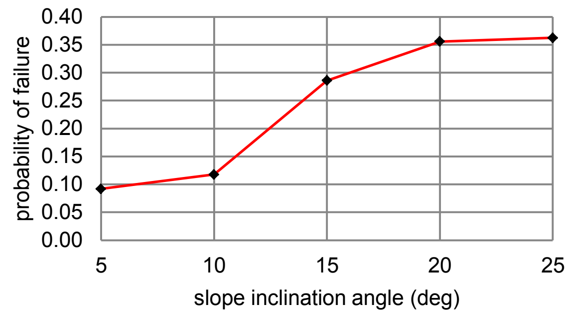

Figure 8. Variation of the probability of failure with the change of slope angle for the worst-case scenario.

Table 4. The slope instability probabilities and the reliability index in terms of θ for the worst-case scenario.

θ (deg)	P(WI)	P(II)	P(F)	β
5	0.09182	0.00007	0.09189	1.33
10	0.09186	0.02572	0.11758	1.19
15	0.09035	0.19562	0.28597	0.57
20	0.08882	0.26712	0.35594	0.37
25	0.08834	0.27395	0.36229	0.35

7 SUMMARY AND CONCLUSIONS

A probabilistic approach for the study of the seismic performance of the slopes of northern Canada was presented. Two modes of instability, weakening and inertial, were considered. Several input parameters related to slope, soil and ground motion were incorporated in the proposed model. The results of the parametric studies showed that:

- The probability of slope failure increases with the increase of slope angle. With this increase, however the contribution of weakening and inertial instabilities changes. Steeper slopes, are more likely to be subjected to inertial instabilities.
- The ground motion parameters, M_w and R, remarkably affect the performance of the slope. The probability of failure has a direct relationship with M_w and an inverse relationship with R. In the case of the studied mild slope, only weakening instabilities were observed, which is not the case for steeper inclination angles.
- The thaw-consolidation conditions, contributing to the excess pore-water pressure prior to seismic excitations, can drastically increase the probability of weakening and inertial instabilities.
- According to the reliability indices obtained from this study, depending on the slope angle and thaw-consolidation conditions, “poor” to “above average” behaviours was predicted for the studied slopes.

8 REFERENCES

Adams, J., Halchuk, S., Allen, T. and Rogers, G. 2015. Canada's 5th Generation Seismic Hazard Model, As Prepared for the 2015 National Building Code of Canada. *11th Canadian Conference on Earthquake Engineering*. Victoria, BC, Canada.

Ambraseys, N.N. and Menu, J.M. 1988. Earthquake-Induced Ground Displacements. *Earthquake Engineering and Structural Dynamics*. 16, 985-1006.

Aylsworth, J.M., Burgess, M.M., Desrochers, D.T., Duk-Rodkin, A., Robertson, T. and Traynor, J.A. 2000. Surficial Geology, Subsurface Materials, and Thaw Sensitivity of Sediments. In *The Physical Environment of the Mackenzie Valley, Northwest Territories: A Base Line for the Assessment of Environmental Change*. *Edited by* L.D. Dyke and G.R. Brooks. Geological Survey of Canada, Bulletin 547. p. 41-48.

Blake, T.F., Hollingsworth, R.A. and Stewart, J.P. 2002. *Recommended Procedures for Implementation of DMG Special Publication 117-Guidelines for Analyzing and Mitigating Landslide Hazards in California*. Southern California Earthquake Center, Los Angeles, CA.

Boore, D.M., Joyner, W.B. and Fumal, T.E. 1997. Equations for Estimating Horizontal Response Spectra and Peak Acceleration from Western North American Earthquakes: A Summary of Recent Work. *Seismological Research Letters*. 68(1): 128-153.

Boulanger, R.W. and Idriss, I.M. 2006. Liquefaction Susceptibility Criteria for Silts and Clays. *Journal of Geotechnical and Geoenvironmental Engineering*. 132(11): 1413-1426.

California Geological Survey. 2008. *Guidelines for Evaluating and Mitigating Seismic Hazards in California*. California Geological Survey Special Publication 117A.

Canadian Commission on Buildings and Fire Codes. 2010. *National Building Code of Canada*. Associate Committee on the National Building Code, National Research Council of Canada, Ottawa, ON, Canada.

Dyke, L. 2000. Stability of Permafrost Slopes in the Mackenzie Valley. In *The Physical Environment of the Mackenzie Valley, Northwest Territories: A Base Line for the Assessment of Environmental Change*. *Edited by* L.D. Dyke and G.R. Brooks. Geological Survey of Canada, Bulletin 547. p. 177-186.

Dyke, L. 2004. Stability of Frozen and Thawing Slopes in the Mackenzie Valley, Northwest Territories. In *57th Canadian Geotechnical Conference, 5th Joint CGS/IAH-CNC Conference*. Quebec, QC, Canada.

Hyndman, R.D., Cassidy, J.F., Adams, J., Rogers, G.C. and Mazzotti, S. 2005. Earthquakes and Seismic Hazard in the Yukon-Beaufort Mackenzie. *CSEG Recorder*.

Ishihara, K. 1993. Liquefaction and Flow Failure During Earthquakes. *Geotechnique*. 43(3): 351-415.

Jibson, R.W. 2007. Regression Models for Estimating Coseismic Landslide Displacement. *Engineering Geology*. 91: 209-218.

Jibson, R.W. and Michael, J.A. 2009. *Maps Showing Seismic Landslide Hazards in Anchorage, Alaska*. U.S. Geological Survey Scientific Investigations Map 3077.

Jibson, R.W., Harp, E.L. and Michael, J.A. 1998. *A Method for Producing Digital Probabilistic Seismic Landslide Hazard Maps, An Example from the Los Angeles, California, Area*. U.S. Geological Survey Open-File Report. 98-113.

Jibson, R.W., Harp, E.L. and Michael, J.A. 2000. A Method for Producing Digital Probabilistic Seismic Landslide Hazard Maps. *Engineering Geology*. 58: 271-289.

Johnston, G.H. 1981. *Permafrost: Engineering, Design and Construction*. John Wiley & Sons, Toronto, ON, Canada.

Joyner, W.B. and Boore, D.M. 1981. Peak Horizontal Acceleration and Velocity from Strong-Motion Records Including Records from the 1979 Imperial Valley, California, Earthquake. *Bulletin of the Seismological Society of America*. 71, 2011-2038.

Keefer, D.K. and Wilson, R.C. 1989. Predicting Earthquake-Induced Landslides, with Emphasis on Arid and Semi-Arid Environments. In *Landslides in a Semi-Arid Environment*. Inland Geological Society, Reverside, CA, Vol. 2, p. 118-149.

Lewkowicz, A.G. 1990. Morphology, Frequency and Magnitude of Active-Layer Detachment Slides, Fosheim Peninsula, Ellesmere Island, N.W.T. In 5*th Canadian Permafrost Conference*. Quebec, QC, Canada.

Lewkowicz, A.G. and Harris, C. 2005. Morphology and Geotechnique of Active-Layer Detachment Failures in Discontinuous and Continuous Permafrost, Northern Canada. *Geomorphology*. 69: 275-297.

Lipovsky, P. and Huscroft, C. 2006. A Reconnaissance Inventory of Permafrost-Related Landslides in the Pelly River Watershed, Central Yukon. Yukon Geological Survey, Whitehorse, YT, Canada.

Mesri, G. 1975. Discussion: New Design Procedure for Stability of Soft Clays. *Journal of the Geotechnical Engineering Division*. 101(GT4): 409-412.

Morgenstern, N.R. and Nixon, J.F. 1971. One-Dimensional Consolidation of Thawing Soils. *Canadian Geotechnical Journal*. 8: 558-565.

Olson, S.M. and Stark, T.D. 2002. Liquefied Strength Ratio from Liquefaction Flow Failure Case Histories. *Canadian Geotechnical Journal*. 39: 629-647.

Phoon, K.K. and Kulhawy, F.H. 1999. Characterization of Geotechnical Variability. *Canadian Geotechnical Journal*. 36: 612-624.

Sarma, S.K. 1988. Seismic Response and Stability of Earth Dams. *Seismic Risk Assessment and Design of Building Structures*. Edited by A. Koridze. Omega Scientific, p. 143–160.

Seed, H.B. and Idriss, I.M. 1971. Simplified Procedure for Evaluating Soil Liquefaction Potential. *Journal of the Soil Mechanics and Foundations Division*. 97: 1249-1273.

US Army Corps of Engineers. 1997. *Engineering and Design Introduction to Probability and Reliability Methods for Use in Geotechnical Engineering*. Technical Letter No. 1110-2-547, Department of the Army, Washington DC, USA.

Uzielli, M., Lacasse, S., Nadim, F. and Phoon, K.K. 2007. Soil Variability Analysis for Geotechnical Practice. In *Characterisation and Engineering Properties of Natural Soils*. Edited by T.S. Tan, K.K. Phoon, D.W. Hight and S. Leroueil, Taylor & Francis Group, London, UK, pp. 1653-1752.

Wang, B., Nichol, S. and Su, X. 2005. Geotechnical Field Observations of Landslides in Fine-Grained Permafrost Soils in the Mackenzie Valley, Canada. In *Landslides, Risk Analysis and Sustainable Disaster Management*. Edited by K. Sassa, H. Fukuoka, F. Wang and G. Wang, Springer, Berlin, Germany, pp. 203-212.

Wieczorek, G.F., Wilson, R.C. and Harp, E.L. 1985. *Map Showing Slope Stability During Earthquakes in San Mateo County, California*. U.S. Geological Survey.

Wilson, R.C. and Keefer, D.K. 1985. Predicting Areal Limits of Earthquake-Induced Landsliding. In *Evaluating Earthquake Hazards in the Los Angeles Region-An Earth-Science Perspective*. Edited by J.I. Ziony. U.S. Geological Survey Professional Paper 1360, pp. 317-345.

Youd, T.L. and Perkins, D.M. 1978. Mapping Liquefaction-Induced Ground Failure Potential. *Journal of Geotechnical Engineering*. 104(4): 433-446.

Youd, T.L., Idriss, I.M., Andrus, R.D., Arango, I., Castro, G., Christian, J.T., Dobry, R., Finn, W.D.L., Harder, L.F., Hynes, M.E., Ishihara, K., Koester, J.P., Liao, S.S.C., Marcuson, W.F., Martin, G.R., Mitchell, J.K., Moriwaki, Y., Power, M.S., Robertson, P.K., Seed, R.B. and Stokoe, K.H. 2001. Liquefaction Resistance of Soils: Summary Report from the 1996 NCEER and 1998 NCEER/NSF Workshops on Evaluation of Liquefaction Resistance of Soils. *Journal of Geotechnical and Geoenvironmental Engineering*. 127: 817-833.

Zhang, Y. 2009. *Impact of Freeze-Thaw on Liquefaction Potential and Dynamic Properties of Mabel Creek Silt*. PhD dissertation, University of Alaska Fairbanks, Fairbanks, AK, USA.